

# Microphase Separation Induced by Differential Interactions in Diblock Copolymer/Homopolymer Blends

Jiajia Zhou\* and An-Chang Shi†

*Department of Physics and Astronomy, McMaster University*

*Hamilton, Ontario, Canada L8S 4M1*

## Abstract

Phase behavior of diblock copolymer/homopolymer blends (AB/C) is investigated theoretically. The study focuses on a special case where all three binary pairs, A/B, B/C and C/A, are miscible. Despite the miscibility of the binary pairs, a closed-loop immiscible region exists in the AB/C blends when the A/C and B/C pair interactions are sufficiently different. Inside the closed-loop, the system undergoes microphase separation, exhibiting different ordered structures. This phenomenon is enhanced when the homopolymer (C) interacts more strongly to one of the blocks (A or B).

arXiv:0906.2205v2 [cond-mat.soft] 18 Jun 2009

---

\*zhouj2@mcmaster.ca

†shi@mcmaster.ca

## I. INTRODUCTION

The development of new polymeric materials is driven by the increasingly complicated requirements of advanced engineering, as well as by the desire to improve material properties and reduce production cost. Beside synthesizing new types of homopolymers and copolymers, blending different polymers provides another route to obtain new materials [1, 2]. Polymer blends can have combinative and enhanced properties of their components. From a thermodynamic point of view, polymer blends may be miscible, partially miscible, or immiscible. The physical properties of polymer blends vary drastically in these different states. From this perspective, a good understanding of the phase behavior of polymer blends is crucial. Because polymer blends are composed of more than one element, their phase behavior is controlled by a large number of parameters, such as chain lengths, monomer interactions and polymer architectures. Due to the very large parameter space, theoretical study is crucially important to understand the phase behavior and material properties in this complex system.

The simplest polymer blend consists of two different homopolymers, A and B. For symmetric binary A/B blends, both homogeneous and inhomogeneous phases exist, depending on the interaction strength  $\chi_{AB}N$ , where  $\chi_{AB}$  is the Flory-Huggins interaction parameter and  $N$  is the degree of polymerization of the polymers [3]. For small values of  $\chi_{AB}N$ , the two homopolymers are miscible and the blend is in a homogeneous state. For  $\chi_{AB}N$  larger than a critical value ( $\chi_{AB}N > 2$ ), the two homopolymers become immiscible. A macrophase separation occurs where the blends separate into A-rich and B-rich phases. The situation is different when the A and B homopolymers are linked together to form AB diblock copolymers. In this case, macrophase separation cannot take place because of the chemical connections between the A and B blocks. Instead, a microphase separation occurs in which the A and B are separated locally at a length scale determined by the size of the polymers [4, 5]. The microphase separation is also controlled by the interaction strength  $\chi_{AB}N$ . For symmetric diblock copolymers, the critical value of  $\chi_{AB}N$  for order-disorder transition is about 10.5.

It is interesting to blend AB diblock copolymers with homopolymers C. In this case the microphase separation of diblock copolymers can compete with the macrophase separation of the homopolymers. The different interactions between different monomers provide a rich

phase behavior. If the homopolymer C is immiscible with both blocks A and B, the situation is simple: the homopolymers will be separated from diblock copolymers. A more complex case involves AB/C blends where the homopolymers C are immiscible with one block of the diblock copolymers, but interact favorably with the other block [6, 7, 8, 9, 10]. This system is similar to the case of amphiphilic molecules in solution, which is important to understand the self-assembly of surfactants and lipids. A simple example of this class of blends is that the homopolymers are chemically identical to one of the blocks of the copolymers, i.e., an AB/A blend. Binary AB/A blends have been extensively studied theoretically [11, 12, 13, 14] and experimentally [15, 16, 17]. The phase diagrams of AB/A blends show the coexistence of macrophase separation and microphase separation, and the addition of the homopolymers tends to stabilize some complex ordered structures.

Another interesting case occurs for blends consisting of C homopolymers that are miscible with both the A and B blocks. The miscible nature of the blends may provide potential applications which rely on the homogeneity of the material. Theoretically and practically, the extension to the attractive interactions between compounds may lead to new phenomena and create new materials. In general, miscible blends are characterized by homogeneous phases. However, phase separation can be induced by differential monomer-monomer interactions. An example is found in ternary blends composed of A/B/C homopolymers where all three binary pairs are miscible. A closed-loop immiscible region is found in the phase diagram [18, 19, 20, 21]. In cases that the attractive interaction between A/C is much stronger than that of B/C and A/B, A and C homopolymers tend to be separated from B. On the other hand, macroscopic phase separation of A and B cannot take place for AB/C blends, because A and B are chemically bonded together. Similar to the case of diblock copolymers, AB/C blends can reduce their free energy through microphase separation. Indeed, the microphase separation of AB/C blends has been observed in experiment of Chen et al. [22]. These authors investigated AB/C blends where the interactions between each pair of segments are favorable. Their experiment revealed a phase diagram with a closed microphase separation loop, despite the fact that the C homopolymers have attractive interactions with both blocks of the copolymers.

In this paper, we present a theoretic study of the phase behavior of diblock copolymer/homopolymer blends. The study focuses on the case where the homopolymers attract to one block much more strongly than to the other block of the diblock copolymers. We use the

Gaussian chain model for the polymers, and apply the random phase approximation (RPA) to examine the stability limits of the homogeneous phase, leading to both macrophase and microphase separation transition. While the RPA calculates the stability boundary of the homogeneous phase, we are also interested in the morphological details inside the microphase separation region. For this purpose, self-consistent field theory is employed. Various representative phase diagrams are constructed to illuminate the general trends in the phase behavior by varying the homopolymer length and monomer-monomer interaction parameters. Comparison with available experiments is given.

## II. RPA ANALYSIS

The system discussed in this work is a mixture of AB diblock copolymers and C homopolymers. For the diblock copolymer, the degrees of polymerization for the A- and B-block are  $Nf_A$  and  $N(1 - f_A)$ , respectively, and the C homopolymers are with a degree of polymerization  $\kappa N$ . The volume fraction of the diblock copolymers and homopolymers in the blends are  $1 - \phi_H$  and  $\phi_H$ , respectively. For simplicity we assume all species have the same monomer volume  $\rho_0^{-1}$  and statistical segment length  $b$ . The interactions between each pair of monomers are characterized by three Flory-Huggins parameters,  $\chi_{AB}$ ,  $\chi_{BC}$  and  $\chi_{AC}$ .

The RPA analysis of the system [3, 4, 23, 24] starts with an external potential  $u_i$  acting on the  $i$  monomer. Assuming that the external fields are small, the density response  $\delta\phi_i$  to the external potential can be written in the Fourier space as a linear function of the external potential,

$$\delta\phi_i(q) = -\beta \sum_j \tilde{S}_{ij}(q) u_j(q), \quad (1)$$

where  $\tilde{S}_{ij}(q)$  is the Fourier transform of the density-density correlation between  $i$  and  $j$  monomers. Here we have used the fact that functions depend on the wave vector  $\mathbf{q}$  only through its magnitude  $q \equiv |\mathbf{q}|$  because of the isotropic symmetry of a homogeneous phase.

The interaction between the monomers can be taken into account through the mean-field approximation. To this end, the effective potential acting on the  $i$  monomer is written in the form,

$$u_i^{\text{eff}}(q) = u_i(q) + \beta^{-1} \sum_{j \neq i} \chi_{ij} \delta\phi_j + \gamma, \quad (2)$$

where the second term accounts for the mean-field interaction between  $i$  and  $j$  monomers,

and  $\gamma$  is a potential required to assure the incompressible condition

$$\sum_i \delta\phi_i(q) = 0. \quad (3)$$

The random phase approximation assumes that the density response  $\delta\phi_i$  is given by the effective potential,

$$\delta\phi_i(q) = -\beta \sum_j S_{ij}(q) u_j^{\text{eff}}(q), \quad (4)$$

where  $S_{ij}(q)$  is the Fourier transform of the density-density correlation when the external potential vanishes.

Equations (1)-(4) form a set of simultaneous equations for the unknowns  $\delta\phi_i$  and  $\gamma$ . By solving these equations, the correlation functions  $\tilde{S}_{ij}$  can be found in terms of  $S_{ij}$  and  $\chi_{ij}$ . The final results are lengthy and details can be found in the work of Ijichi and Hashimoto[24].

The free energy of AB/C blends can be written as a Landau expansion about the homogeneous state in terms of the density fluctuations  $\delta\phi_i$ ,

$$\begin{aligned} \frac{F - F_{\text{hom}}}{(\rho_0 V / \beta N)} &= \frac{1}{2!(2\pi)} \int \tilde{S}_{ij}^{-1}(q) \delta\phi_i(q) \delta\phi_j(-q) dq + \dots, \\ &= \frac{1}{2!(2\pi)} \int \lambda_k(q) |\delta\psi_k(q)|^2 dq + \dots, \end{aligned} \quad (5)$$

where  $\tilde{S}_{ij}^{-1}(q)$  is the inverse of the correlation function  $\tilde{S}_{ij}(q)$ . Here we have neglected terms with order higher than two, and the second-order term can be further written in a quadratic form, where  $\lambda_k(q)$  are eigenvalues of matrix  $\tilde{S}_{ij}^{-1}(q)$ . The stability of the homogeneous phase depends on the sign of eigenvalues  $\lambda_k(q)$ . When  $\lambda_k(q) > 0$ , the contribution of any fluctuations to the free energy is always positive, so the homogeneous phase is stable. When  $\lambda_k(q) < 0$ , the fluctuations reduce the free energy and the homogeneous phase is unstable.

Normally, the inverse of the correlation function  $\tilde{S}_{ij}^{-1}(q)$  is a  $3 \times 3$  matrix for the AB/C blends. The incompressible condition reduces the order of the matrix by one. The spinodal line is determined by the condition that the smaller eigenvalue goes to zero. Typical plots of  $\lambda_k(q)$  are shown in Figure 1. In general, one of the eigenvalues  $\lambda_1(q)$  is always positive, while the other one  $\lambda_2(q)$  approaches zero when  $\chi_{AC}N$  changes.

The macrophase separation is characterized by  $\lambda_2(q) \rightarrow 0$  at  $q = 0$ . This is shown in Figure 1(a) for blends with  $\kappa = 1.0$ ,  $f_A = 0.8$ ,  $\phi_H = 0.2$ ,  $\chi_{AB}N = 15$ ,  $\chi_{BC}N = 0$  and different  $\chi_{AC}N$  values. The eigenvalue  $\lambda_2(q)$  has a minimum at  $q = 0$ , and the minimum value approaches zero when  $\chi_{AC}N$  increases. When  $\lambda_2(q)$  becomes negative, any small

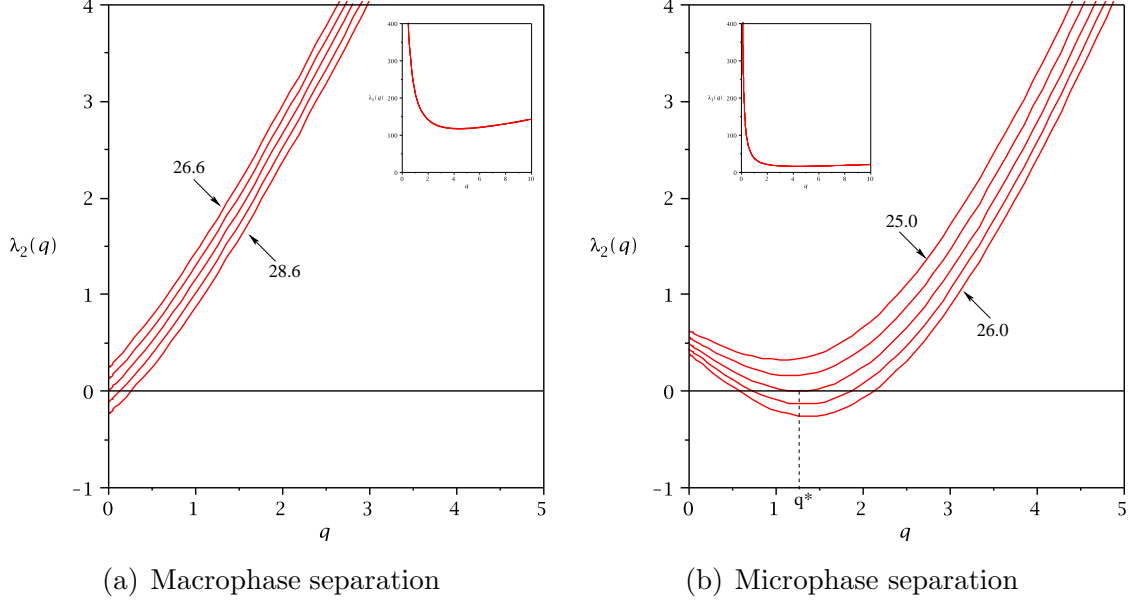


FIG. 1: Plots of eigenvalues  $\lambda_k(q)$  for (a)  $\kappa = 1.0$ ,  $f_A = 0.2$ ,  $\phi_H = 0.8$ ,  $\chi_{AB}N = 15$ ,  $\chi_{BC}N = 0$  and a range of  $\chi_{AC}N$  values ( $26.6 \sim 28.6$ ), and (b)  $\kappa = 1.0$ ,  $f_A = 0.2$ ,  $\phi_H = 0.2$ ,  $\chi_{AB}N = 15$ ,  $\chi_{BC}N = 0$  and a range of  $\chi_{AC}N$  values ( $25.0 \sim 26.0$ ). The insets show the positive eigenvalue  $\lambda_1(q)$ . Variations of  $\lambda_2(q)$  with  $\chi_{AC}N$  are shown, but they are not visible for  $\lambda_1(q)$ . The unit of the wave vector  $q$  is  $R_g^{-1}$ , where  $R_g = \sqrt{Nb^2/6}$  being the radius of gyration.

density fluctuations with  $q = 0$  decrease the free energy, leading to a growth of fluctuations with macroscopic wavelength. This corresponds to a macrophase separation between the diblock-rich phase and homopolymer-rich phase.

On the other hand, the diblock copolymers in the blend introduce the possibility of microphase separation. A microphase transition is characterised by the eigenvalue  $\lambda_2(q) \rightarrow 0$  at some finite  $q^* > 0$ . This is shown in Figure 1(b) for blends with  $\kappa = 1.0$ ,  $f_A = 0.2$ ,  $\phi_H = 0.2$ ,  $\chi_{AB}N = 15$ ,  $\chi_{BC}N = 0$  and different  $\chi_{AC}N$  values. The Fourier mode with nonzero wave number  $q^*$  becomes unstable upon increasing  $\chi_{AC}N$ , leading to the formation of ordered structure with length scale of  $(q^*/2\pi)^{-1}$ . This is in contrast to Figure 1(a) where the Fourier mode  $q = 0$  is destabilized first.

The six parameters  $(\kappa, f_A, \phi_H, \chi_{AB}N, \chi_{BC}N, \chi_{AC}N)$  characterising the AB/C blends lead to a huge phase space. Some restrictions are needed so that the phase behavior can be described. We will keep  $\kappa = 1.0$  for the RPA calculation, which means the homopolymer C has the same degree of polymerization as the diblock copolymer AB. Furthermore, we will

assume  $\chi_{BC}N = 0$ , which represents the case where the A/C interaction is much stronger than the B/C interaction.

Figure 2(a) shows a typical phase diagram in the  $\phi_H$ - $\chi_{AC}N$  plane. The parameters are  $f_A = 0.2$  and  $\chi_{AB}N = 2$ . The solid lines and dotted lines represent, respectively, the stability limits for the macrophase separation transition  $(\chi_{AC}N)_{\text{macro}}$  and microphase separation transition  $(\chi_{AC}N)_{\text{micro}}$ .

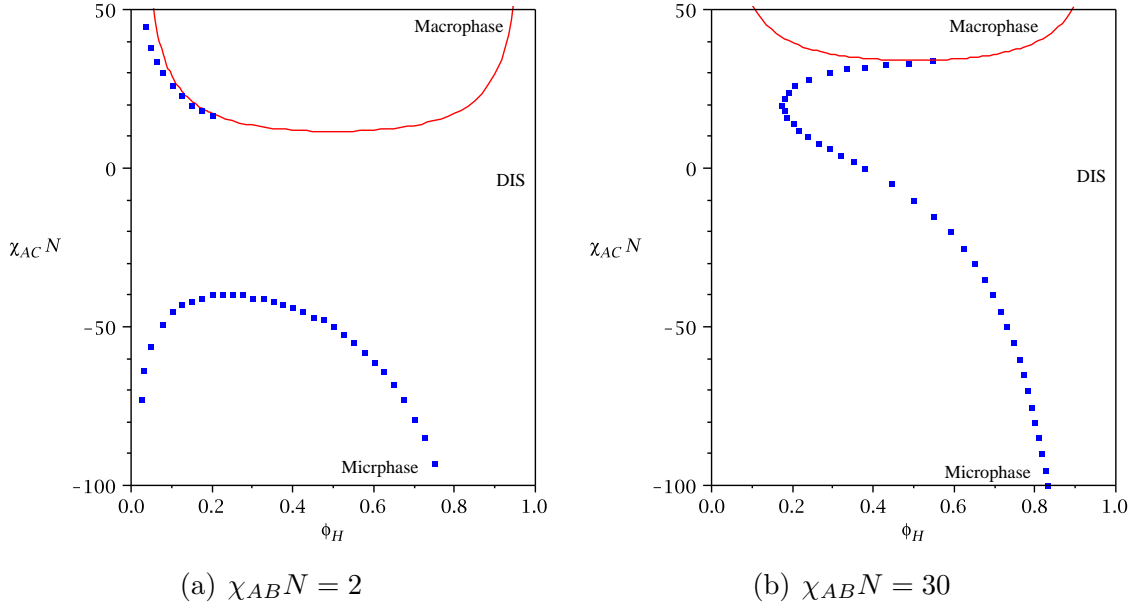


FIG. 2: Phase diagrams for blends with parameters  $\kappa = 1.0$ ,  $f_A = 0.2$ ,  $\chi_{BC}N = 0$  and (a)  $\chi_{AB}N = 2$ , (b)  $\chi_{AB}N = 30$ . The solid and dotted lines represent the stability limits for macrophase and microphase separation transition, respectively. Regions of macrophase separation, microphase separation and disordered states are labeled by Macrophase, Microphase and DIS.

The blends are disordered around  $\chi_{AC}N = 0$  and  $\phi_H = 1$ , and ordered phases appear at both  $\chi_{AC}N > 0$  and  $\chi_{AC}N < 0$ . In the region where  $\chi_{AC}N > 0$ , increasing  $\chi_{AC}N$  induces an instability to either macrophase separation or microphase separation, depending on the blend composition and copolymer asymmetry. For blends with a minority of homopolymers, microphase separation occurs first when  $\chi_{AC}N$  is increased. However, when the composition of the homopolymers increases to certain value, the blend undergoes macrophase separation when  $\chi_{AC}N$  is increased. The critical composition for blends with  $f_A = 0.2$  is  $\phi_H \approx 0.2$ . The shape of the stability lines also suggests that, for small  $\phi_H$  value, both  $(\chi_{AC}N)_{\text{macro}}$  and  $(\chi_{AC}N)_{\text{micro}}$  decrease with increasing  $\phi_H$ , while  $(\chi_{AC}N)_{\text{macro}}$  increases with increasing  $\phi_H$ .

at large  $\phi_H$  value. The former case suggests that the composition of the diblock copolymer in the blend suppresses the phase transition, which is known as the compatibilizing effect of the block polymers [25].

On the other hand, the microphase separation also occurs in the region where  $\chi_{AC}N$  is negative. Since the interaction between the blocks  $\chi_{AB}N = 2$ , the pure diblock copolymers are in the disordered state. The stability line for the microphase separation approaches  $\phi_H = 0$  axis infinitely close when  $\chi_{AC}N$  has a large negative value. It is interesting that for a homogeneous diblock copolymer melt, adding a small amount of homopolymers C which has a strong attractive interaction with one of the blocks will induce the phase separation. Upon increasing  $\phi_H$ ,  $(\chi_{AC}N)_{\text{micro}}$  increases sharply at first, then decreases after  $\phi_H \approx 0.25$ .

A similar phase diagram for blends with  $\chi_{AB}N = 30$  is shown in Figure 2(b). In this case, the pure diblock copolymers are in the ordered state. This leads to the convergence of the two microphase separation regions at  $\chi_{AC}N > 0$  and  $\chi_{AC}N < 0$ .

Another perspective to understand the phase transition is to plot the phase diagram in the  $\phi_H$ - $f_A$  plane for fixed interaction parameters. Figure 3 shows phase diagrams for blends with  $\chi_{AB}N = 2$  and different values of  $\chi_{AC}N$ . They can be viewed as cross-sections pictures of Figure 2(a) at different values of  $\chi_{AC}N$ . At  $\chi_{AC}N = 30$ , because of the strong repelling interaction between A/C, large region of macrophase separation exists, while a small region of microphase separation occurs near the  $\phi_H = 0$  axis. As  $\chi_{AC}N$  decreases, the macrophase separation region shrinks and eventually disappears at negative value of  $\chi_{AC}N$ . At the same time, a closed-loop microphase separation region appears, as can be seen from Figure 3(c) and 3(d). Qualitatively, this closed immiscible loop corresponds to the one observed in experiments [22].

### III. SELF-CONSISTENT FIELD THEORY

Because of its simplicity, random phase approximation provides a convenient method to calculate the order-disorder transition for various parameter sets, but it is difficult to apply RPA to the order-order transition. On the other hand, self-consistent field theory has been proven a powerful method to determine the microstructures of polymer blends [12, 13, 14, 26, 27, 28]. Therefore, it is desirable to apply self-consistent field theory to the study of the phase behavior of AB/C blends.

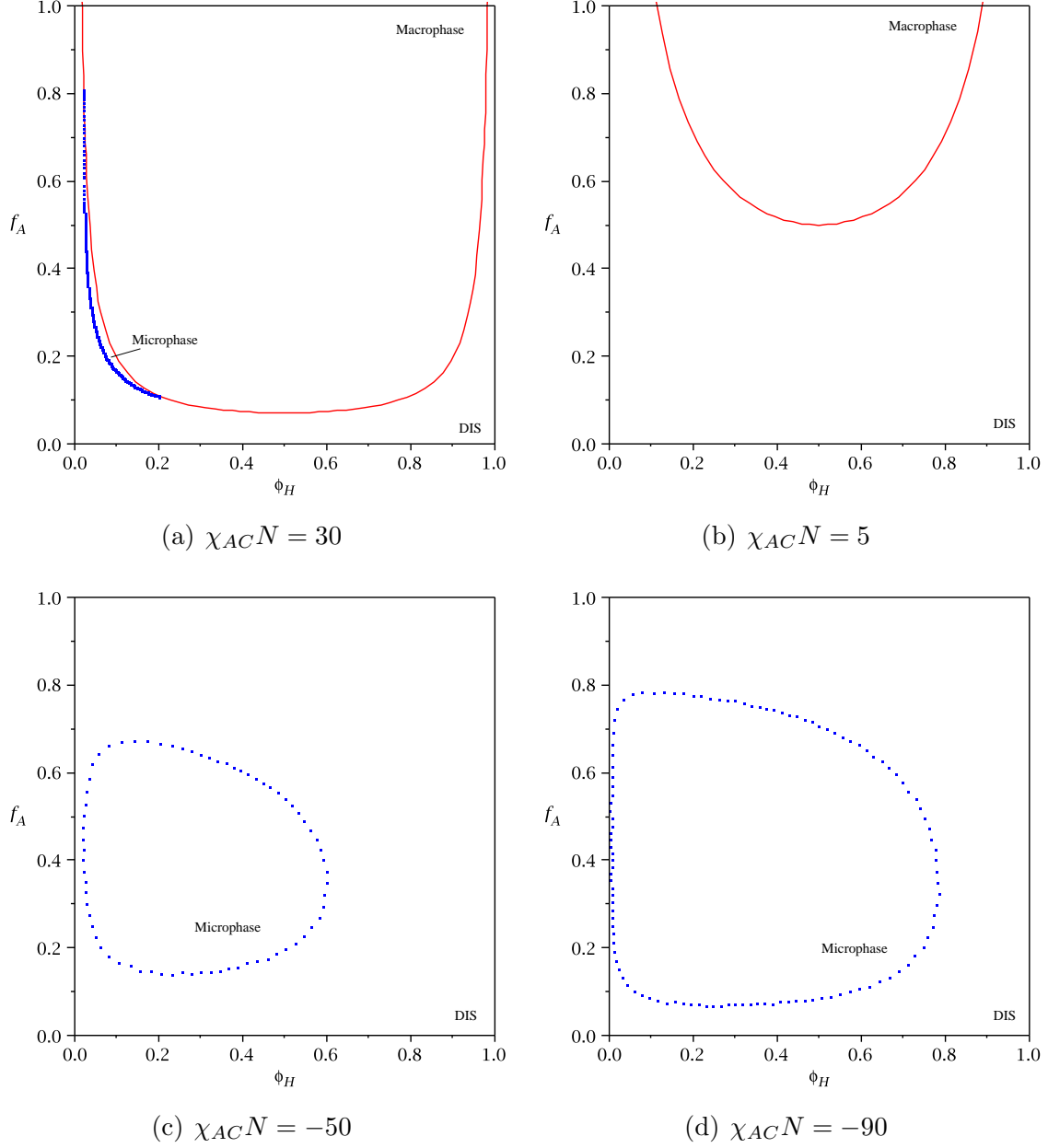


FIG. 3: Phase diagrams for AB/C blends in  $\phi_H$ - $f_A$  plane. The parameters are  $\kappa = 1.0$ ,  $\chi_{AB}N = 2$  and  $\chi_{BC}N = 0$ . The solid and dotted lines represent the transitions for macrophase and microphase separation, respectively.

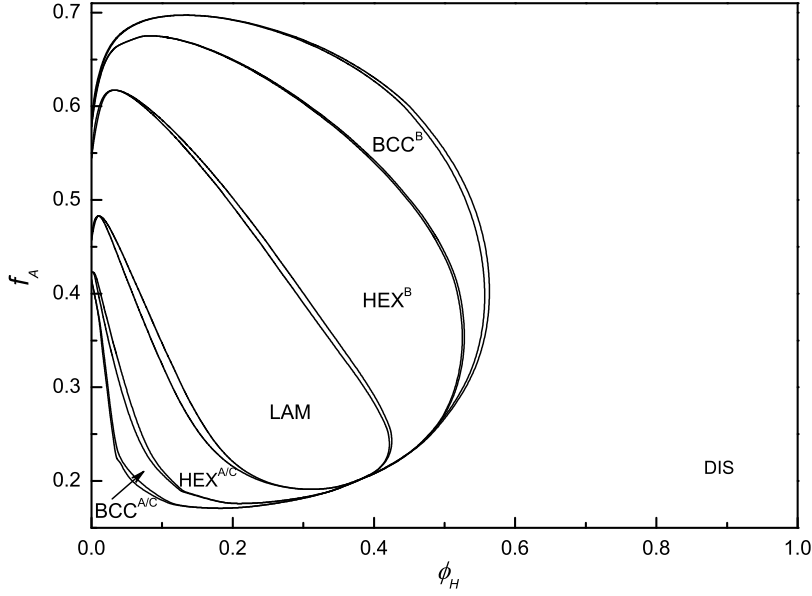
In the framework of self-consistent field theory, the system that consists of many interacting diblock copolymer/homopolymer chains is replaced by the problem of an ideal Gaussian chain in an averaged effective mean-field potential which depends on the position of the chain. Once the mean-field potential is specified, the thermodynamics properties of the system, such as the partition function and monomer densities, can be expressed in terms of

the chain propagators, which are related to the potential by a modified diffusion equations. From the monomer densities, a new mean-field potential can be constructed. The procedure results a closed set of equations that can be solved self-consistently using numerical methods. Once the self-consistent solutions are reached, the free energy can be estimated for various ordered structures. A phase diagram is constructed by finding the morphology with the lowest free energy. In this work, the calculation is performed in the grand-canonical ensemble, and the self-consistent equations are solved using the spectral method [26, 27, 29].

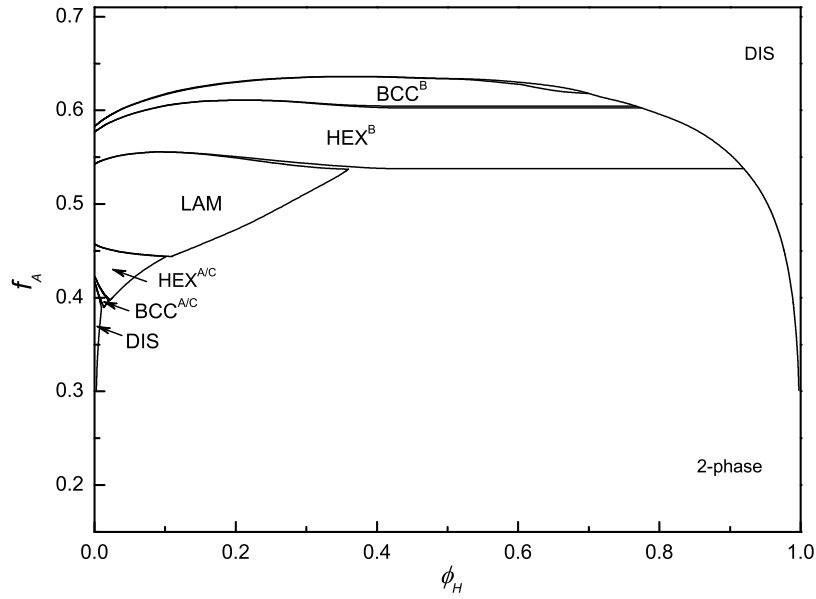
For simplicity, we consider only the classical phases in the current study: lamellae (LAM), cylinders on a hexagonal lattice (HEX), and spheres on a body-centered cubic lattice (BCC). Complex structures, such as close-packed spheres, perforated lamellae and bi-continuous cubic phases, can also occur for certain parameters [12]. These non-classical phases were found only in narrow regions between the classical phases. In this study, we are more interested in the evolution of the phase diagram by varying different parameters, therefore we restrict ourselves to the three classical phases.

Figure 4(a) shows a phase diagram in the  $\phi_H$ - $f_A$  plane for blends with  $\kappa = 1.0$ ,  $\chi_{AB}N = 11$ ,  $\chi_{BC}N = 0$  and  $\chi_{AC}N = -30$ . In this case, the value of  $\chi_{AB}N$  is large enough so the diblock copolymer melt is in an ordered state. The results should converge to the pure diblock results as the homopolymer concentration goes to zero, which is the case as shown in Figure 4(a). The phase behavior shown in Figure 4(a) is typical for the case where the homopolymers attract strongly to one of the blocks ( $\chi_{AC}N = -30$ ). This attractive interaction drives the C homopolymers to the A-domains, leading to larger regions of ordered phases for mediated homopolymer concentrations. For comparison, a phase diagram for the blends with  $\kappa = 1.0$ ,  $\chi_{AB}N = 11$ ,  $\chi_{BC}N = 12$  and  $\chi_{AC}N = 0$  is presented in Figure 4(b). Here the parameters are chosen in such a way that the C monomers accumulate inside the A-rich region for both cases. Figure 4(b) is similar to the results of AB/A blends from Matsen [13] because the interaction parameters  $\chi_{AB}N$  and  $\chi_{BC}N$  are close to each other, thus the system resembles the AB/A blends.

These two phase diagrams display similar features when the homopolymer concentration is small. In this region, the majority of the blend is diblock copolymers and adding small amount of homopolymers should preserve the morphologies. When the homopolymer concentration becomes large, these two phase diagrams exhibit different phase behavior. For the case shown in Figure 4(b), where the interaction parameter  $\chi_{BC}N$  is positive, two possible



(a)  $\chi_{AC}N = -30$



(b)  $\chi_{AC}N = 12$

FIG. 4: Phase diagrams of AB/C blends with parameters  $\kappa = 1.0$ ,  $\chi_{AB}N = 11$ ,  $\chi_{BC}N = 0$ , and (a)  $\chi_{AC}N = -30$ , (b)  $\chi_{AC}N = 12$ . The superscripts of HEX and BCC phase denote the components that form the cylinders and spheres near the lattice centers. There are regions of 2-phase coexistence between the ordered phases.

scenarios of phase behavior appear. When  $f_A$  is large, only one disordered phase is stable. The blend tends to undergo unbinding transition where the spacing of the ordered structure increases and eventually diverges at certain homopolymer concentration [12, 13, 14]. When  $f_A$  is small, macroscopic phase separation becomes an option. Adding more homopolymers induces a macrophase separation transition, in which the blend separates into copolymer-rich and homopolymer-rich regions. On the other hand, for the case shown in Figure 4(a), where  $\chi_{AC}N$  has a large negative value, only one disordered phase is permitted. When the homopolymer concentration is large, the blends exhibit neither the unbinding transition nor the macrophase separation. This behavior is due to the strong attractive interaction between the A and C monomers. As the homopolymer concentration is increased close to unity, both cases reach a disordered phase.

When all three binary pairs are miscible, the AB/C blends exhibit another type of phase behavior. Figure 5 shows a typical phase diagram for this case with  $\kappa = 1.0$ ,  $\chi_{AB}N = 2$ ,  $\chi_{BC}N = 0$  and  $\chi_{AC}N = -40$ . In this case the blends are in a disordered phase at  $\phi_H = 0$  and  $\phi_H = 1$ . Ordered phases occur in a closed-loop region, as indicated by the RPA analysis. Inside the closed-loop, different ordered structures are found. The order-order transitions between these structures are controlled largely by the homopolymer concentration  $\phi_H$ .

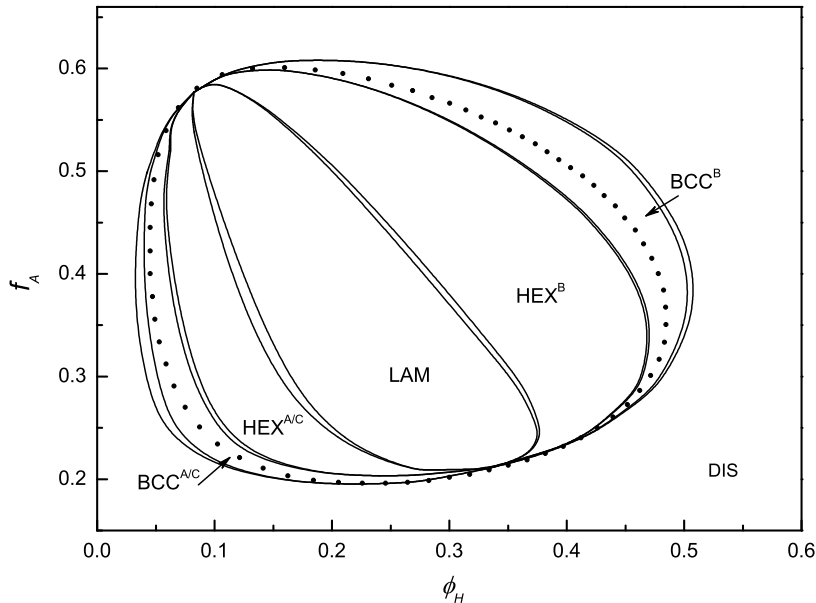


FIG. 5: Phase diagram of AB/C blends with parameters  $\kappa = 1.0$ ,  $\chi_{AB}N = 2$ ,  $\chi_{BC}N = 0$  and  $\chi_{AC}N = -40$ . The dotted line shows the RPA result.

There are two critical points at which all ordered phases converge on the order-disorder transition boundary. For the parameters used here, one point is located at  $(\phi_H = 0.083, f_A = 0.58)$ , and the other one at  $(\phi_H = 0.33, f_A = 0.21)$ . The order-disorder transition is a second-order transition at these two critical points, while the transition is first-order elsewhere. The nature of the order-disorder transition (ODT) can be understood by considering the third-order term in the free energy expansion. A first-order phase transition occurs when a non-zero third-order term is present. In the case of a phase transition from the disordered phase to the BCC phase, the third-order term does not vanish in general. Therefore a first-order ODT is expected. At the critical points, the ODT corresponds to a direct transition from the disordered phase to a lamellar phase. In this case the symmetry of the lamellar phase ensures the vanishment of the third-order term, resulting in a second-order ODT [30].

It is important to point out the limitation of the present theory. The mean-field approach used here approximates the fluctuating potential by a thermal averaged potential. This assumption becomes inaccurate near the order-disorder transition, where the fluctuations are large. The fluctuations can shift the position of the phase boundary, and may change the second-order ODT into a weakly first-order transition [31, 32].

When the homopolymer concentration is increased, the AB/C blends change from a disordered phase to BCC, HEX and LAM phases. This sequence of phase transition can be understood by examining how homopolymers are distributed in the diblock melt. Since the interaction between A and B are at  $\chi_{AB}N = 2$ , which is well below the ODT value of 10.5 for symmetric diblocks, the pure diblock copolymers are in a disordered state. When small amount of homopolymers are added to the system, due to their strong attraction to A-blocks, the homopolymers are distributed around the A-blocks, resulting in an effective segregation of the A-B blocks. Ordered phases emerge when this effective segregation becomes strong enough. Another way to picture this effect is to take the homopolymers as the core-forming agents of micelles in a diblock copolymer melt. The appearance of the spherical phase as the homopolymers are added can be regarded as the ordering of these micelles. The key observation here is that the reduction of interaction energy from A-C segregation is sufficient to overcome the entropy loss. At the strong-segregation limit, a similar mechanism for the formation of reverse structures has been discussed by Semenov [11].

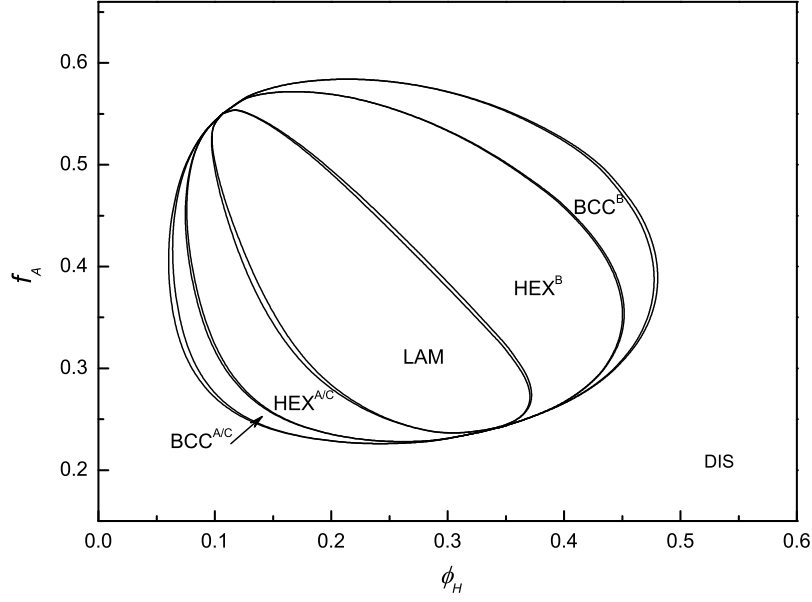
At higher homopolymer concentration, the volume of A/C domain increases. The packing requirement of larger A/C domains leads to a change of the interfaces between A/C and

B, such that the interfaces are curved more towards the B-domain. This mechanism lead to order-order phase transitions from BCC to HEX, and then from HEX to LAM phases. After the LAM structure, adding more homopolymers induces the phase transition to HEX, and then to BCC, where the HEX and BCC both have B-blocks as the central components. Eventually, a disordered phase is reached when sufficient amount of homopolymers are added.

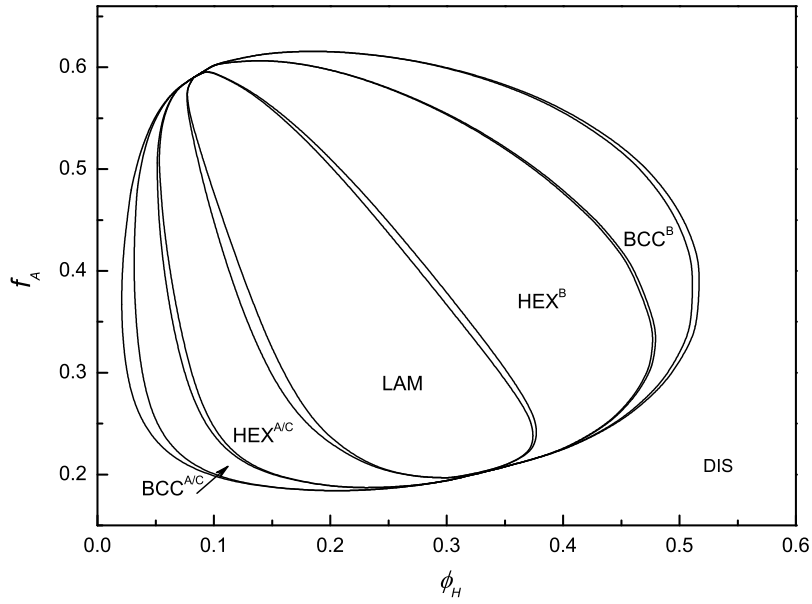
In order to explore the effect of the A/C interactions, phase diagrams are constructed for different A/C interactions, either by changing the molecular-weight of C homopolymers or by changing the value of the Flory-Huggins parameter  $\chi_{AC}$ . Figure 6(a), 5 and 6(b) show the evolution of the phase diagrams with increasing  $\kappa$  ( $\kappa = 0.5, 1.0$  and  $1.5$ ). Alternatively, the phase diagrams in Figure 7(a), 5 and 7(b) demonstrate the progression as  $\chi_{AC}N$  decreases ( $\chi_{AC}N = -35, -40$  and  $-45$ ) at fixed  $\kappa$ . It is obvious that the qualitative feature of the phase diagram stays the same in these phase diagrams. The main difference is the size of the closed-loop ordered phase region. Increasing the interaction will increase the area of the parameter space in which the blend is ordered.

Experimentally, several groups had studied blends with attractive interactions [22, 33]. In Ref. [22], Chen et al. studies the phase diagrams of poly(vinylphenol-*b*-methyl methacrylate)/ poly(vinylpyrrolidone) (PVPh-*b*-PMMA/PVP) blends, where all three binary pairs, PVPh/PMMA, PMMA/PVP and PVP/PVPh, are miscible. Their setup closely resembles the blends studied in this work. They found a closed-loop microphase separation region surrounded by disordered phases. The three classical phases were also observed inside the closed-loop. The position of the closed-loop is similar to our theoretical prediction. Furthermore, the transition sequence of ordered phases from their experiments is consistent with our theoretical phase diagrams.

In a slightly different experiment setup [33], Tirumala et al. studied a poly(oxyethylene-oxypropylene-oxyethylene) triblock copolymer/poly(acrylic acid) blend (PEO-PPO-PEO/PAA), where PAA interacts selectively to the end-block PEO. Upon increasing homopolymer concentration, they observed a phase sequence of disordered phase to lamellae, then to cylinders consisted of PPO, then back to disordered phase. This transition sequence is again consistent with our theoretical predictions.

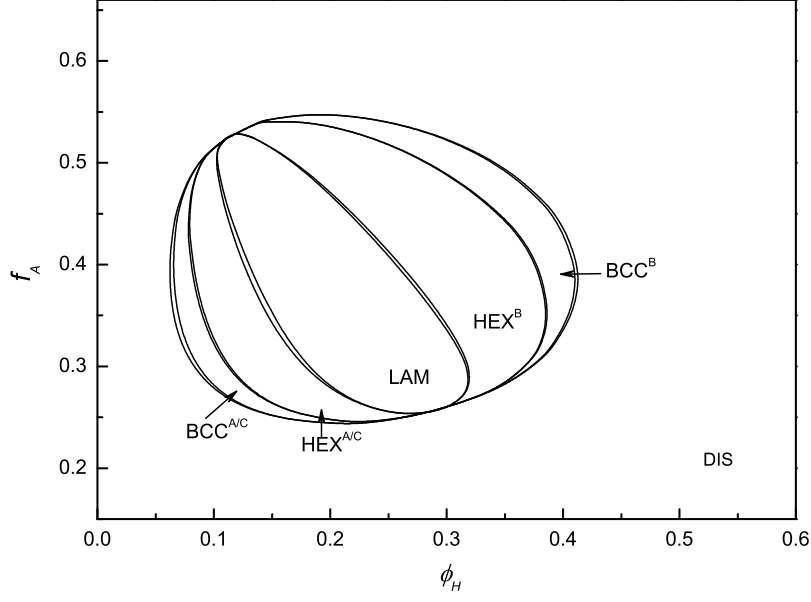


(a)  $\kappa = 0.5$

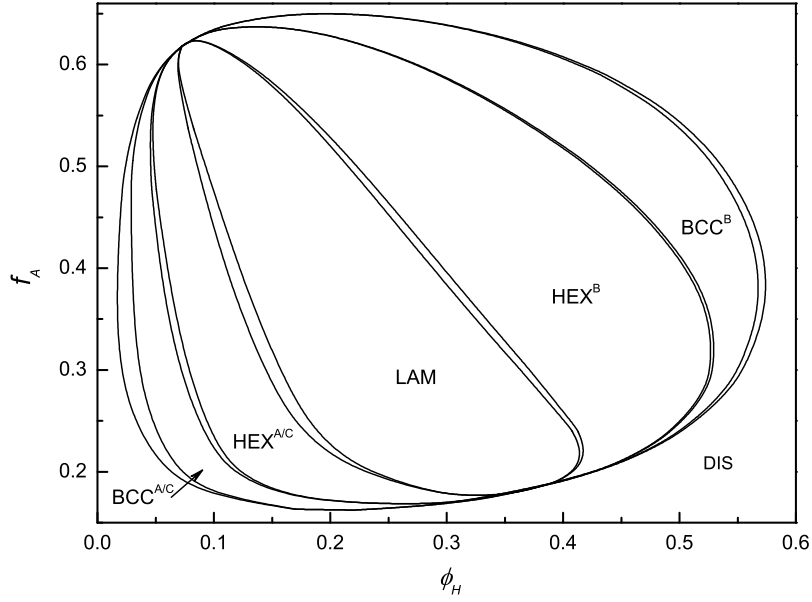


(b)  $\kappa = 1.5$

FIG. 6: Phase diagrams of AB/C blends with parameters  $\chi_{AB}N = 2$ ,  $\chi_{BC}N = 0$ ,  $\chi_{AC}N = -40$  and (a)  $\kappa = 0.5$ , (b)  $\kappa = 1.5$ .



(a)  $\chi_{AC}N = -35$



(b)  $\chi_{AC}N = -45$

FIG. 7: Phase diagrams of AB/C blends with parameters  $\kappa = 1.0$ ,  $\chi_{AB}N = 2$ ,  $\chi_{BC}N = 0$ , and (a)  $\chi_{AC}N = -35$ , (b)  $\chi_{AC}N = -45$ .

#### IV. SUMMARY

In this paper, we have investigated the phase behavior of blends composed of AB diblock copolymers and C homopolymers. Two theoretical methods have been employed to construct the phase diagrams. By using the random phase approximation, the stability limits of the homogeneous phase are obtained. The phase diagrams are characterized by the coexistence of macrophase separation and microphase separation. When the interaction between A/C is repulsive, increasing  $\chi_{AC}N$  will induce the transition from disordered phase to ordered phase, and the property of the transition depends on the homopolymer concentration. In general, blends with low homopolymer concentration tend to undergo microphase separation transition, whereas macrophase separation occurs at high homopolymer concentration. When the interaction parameter  $\chi_{AC}N$  becomes attractive, the macrophase separation disappears while the microphase separation can still occur when the magnitude of  $\chi_{AC}N$  is large. The microphase separation is caused by the strong attraction between the homopolymers to one of the blocks of the diblock copolymers. The difference between the A/C and B/C interactions leads to the spatial separation of B monomers from the A/C monomers, but the chemical connections between A and B prevent the macrophase separation. The microphase separation manifests itself in the  $\phi_H$ - $f_A$  phase diagram in a closed-loop region.

The detailed morphologies inside the closed-loop are calculated using self-consistent field theory. The RPA results provide a guidance to explore the parameter space. Three classical ordered phases (LAM, HEX and BCC) are included in the current study. Along the closed-loop, the microphase separation transition is a first-order phase transition from disordered phase to the microphase with the symmetry of a body-centered cubic lattice except at two critical points. At these two points, the mean-field approach indicates that the blends undergo continuous phase transition from disordered phase to lamellar phase. When the homopolymer concentration is low, the phase sequence upon increasing homopolymer concentration is from BCC to HEX, and from HEX to LAM. At high homopolymer concentration, the phase sequence is reversed.

Another interesting observation of the phase diagram is the reverse morphology where the majority component of the diblock forms the dispersed domains of the ordered structure when small amount of homopolymers are added into the diblock melts. This phenomenon is due to the fact that the attractive interaction of A/C is much stronger than that of B/C.

The closed-loop microphase separation region has been observed in experiment [22], and our theoretical prediction is in qualitative agreement with the experimental result. Phase diagrams for blends with different homopolymer lengths and Flory-Huggins parameters are also presented. It is observed that varying the interaction changes the size of the closed-loop, while the general features of the phase diagram are preserved.

### Acknowledgments

This work was supported by the Natural Sciences and Engineering Research Council (NSERC) of Canada. The computation was made possible by the facilities of the Shared Hierarchical Academic Research Computing Network (SHARCNET:www.sharcnet.ca).

- 
- [1] D. Paul and S. Newman, eds., *Polymer Blends* (Academic Press, New York, 1978).
  - [2] L. Utracki, *Polymer Alloys and Blends: Thermodynamics and Rheology* (Hanser Pub, New York, 1989).
  - [3] P.-G. de Gennes, *Scaling Concepts in Polymer Physics* (Cornell University Press, Ithaca, 1979).
  - [4] L. Leibler, *Macromolecules* **13**, 1602 (1980).
  - [5] I. Hamley, *The Physics of Block Copolymers* (Oxford University Press, Oxford, 1998).
  - [6] M. Jiang and H. Xie, *Prog. Polym. Sci.* **16**, 977 (1991).
  - [7] M. Jiang, T. Huang, and J. Xie, *Macromol. Chem. Phys.* **196**, 787 (1995).
  - [8] B. Löwenhaupt, A. Steurer, G. Hellmann, and Y. Gallot, *Macromolecules* **27**, 908 (1994).
  - [9] J. Zhao, E. Pearce, and T. Kwei, *Macromolecules* **30**, 7119 (1997).
  - [10] Y. Han, E. Pearce, and T. Kwei, *Macromolecules* **33**, 1321 (2000).
  - [11] A. Semenov, *Macromolecules* **26**, 2273 (1993).
  - [12] M. Matsen, *Phys. Rev. Lett.* **74**, 4225 (1995).
  - [13] M. Matsen, *Macromolecules* **28**, 5765 (1995).
  - [14] P. Janert and M. Schick, *Macromolecules* **31**, 1109 (1998).
  - [15] T. Hashimoto, H. Tanaka, and H. Hasegawa, *Macromolecules* **23**, 4378 (1990).
  - [16] H. Tanaka, H. Hasegawa, and T. Hashimoto, *Macromolecules* **24**, 240 (1991).

- [17] K. Winey, E. Thomas, and L. Fetters, *Macromolecules* **24**, 6182 (1991).
- [18] L. Zeman and D. Patterson, *Macromolecules* **5**, 513 (1972).
- [19] W. Jo, Y. Kwon, and I. Kwon, *Macromolecules* **24**, 4708 (1991).
- [20] C. Manestrel, D. Bhagwagar, P. Painter, M. Coleman, and J. Graf, *Macromolecules* **25**, 1701 (1992).
- [21] S.-W. Kuo, C.-L. Lin, and F.-C. Chang, *Macromolecules* **35**, 278 (2002).
- [22] W.-C. Chen, S.-W. Kuo, U.-S. Jeng, and F.-C. Chang, *Macromolecules* **41**, 1401 (2008).
- [23] K. Mori, H. Tanaka, and T. Hashimoto, *Macromolecules* **20**, 381 (1987).
- [24] Y. Ijichi and T. Hashimoto, *Polym. Commun.* **29**, 135 (1988).
- [25] H. Tanaka and T. Hashimoto, *Polym. Commun.* **29**, 212 (1988).
- [26] M. Matsen and M. Schick, *Phys. Rev. Lett.* **72**, 2660 (1994).
- [27] A.-C. Shi, in *Developments in Block Copolymer Science and Technology*, edited by I. Hamley (John Wiley & Sons, New York, 2004), chap. 8.
- [28] G. H. Fredrickson, *The Equilibrium Theory of Inhomogeneous Polymers* (Clarendon Press, Oxford, 2006).
- [29] M. Laradji, A.-C. Shi, R. Desai, and J. Noolandi, *Phys. Rev. Lett.* **78**, 2577 (1997).
- [30] R. Wang, W. Li, Y. Luo, B.-G. Li, A.-C. Shi, and S. Zhu, *Macromolecules* **42**, 2275 (2009).
- [31] G. H. Fredrickson and E. Helfand, *J. Chem. Phys.* **87**, 697 (1987).
- [32] L. Kielhorn and M. Muthukumar, *J. Chem. Phys.* **107**, 5588 (1997).
- [33] V. Tirumala, V. Daga, A. Bosse, A. Romang, J. Ilavsky, E. Lin, and J. Watkins, *Macromolecules* **41**, 7978 (2008).

\*\*\*

— *Copyright 2009 American Institute of Physics. This article may be downloaded for personal use only. Any other use requires prior permission of the author and the American Institute of Physics.*

— *The following article appeared in *J. Chem. Phys.* **130**, 234904 (2009) and may be found at <http://link.aip.org/link/?JCPSA6/130/234904/1>.*